DISSERTATION ON

RADIOLOGICAL EVALUATION OF PRIMARY BRAIN TUMOURS USING COMPUTED TOMOGRAPHY AND MAGNETIC RESONANCE IMAGING

Submitted in partial fulfillment of the requirements for

M.D. DEGREE – BRANCH–VIII - RADIODIAGNOSIS

OF

THE TAMILNADU DR. M.G.R. MEDICAL UNIVERSITY
CHENNAI

MADRAS MEDICAL COLLEGE

CHENNAI-600 003.

MARCH 2007

CERTIFICATE

This is to certify that dissertation entitled ***"RADIOLOGICAL EVALUATION OF PRIMARY BRAIN TUMOURS USING COMPUTED TOMOGRAPHY AND MAGNETIC RESONANCE IMAGING****" submitted by* ***Dr. C. NELLAIAPPAN*** *appearing for MD (Branch - VIII) Radio Diagnosis Examination in March 2007 is a bonafide work done by him under my direct guidance and supervision in partial fulfillment of regulations of the Tamilnadu Dr.MGR medical university, Chennai. I forward this to the Tamilnadu Dr.MGR Medical University Chennai, Tamil Nadu, India.*

Signature of the Guide & HOD
Prof.V.CHANDRASEKHAR MDRD,DMRD
Head of the department,
Barnard Institute of Radiology
Madras Medical College
Chennai-600 003.

Signature of the Director
Prof. T.S. SWAMINATHAN MD,DMRD
Director
Barnard Institute of Radiology
Madras Medical College
Chennai-600 003.

DEAN
Madras Medical College,
Govt. General Hospital,
Chennai- 600 003.

DECLARATION

I declare that this dissertation titled "**RADIOLOGICAL EVALUATION OF PRIMARY BRAIN TUMOURS USING COMPUTED TOMOGRAPHY AND MAGNETIC RESONANCE IMAGING"** has been conducted by me under the guidance and supervision of Dr.V.Chandrasekhar MD,DMRD, Head of Department, Barnard Institute Of Radiology, Madras Medical College, Chennai.

It is submitted in part of fulfillment of the requirement of award of MD (Branch - VIII) Radio Diagnosis – March 2007 to be held under the Tamil Nadu Dr.M.G.R. Medical University, Chennai. This has not been submitted previously by me for award of any Diploma or Degree in any other University.

Dr. C. Nellaiappan
Postgraduate M.D., Radio Diagnosis
Barnard Institute of Radiology,
Madras Medical College,
Chennai- 600 003.

Acknowledgement

I express my sincere gratitude to **Prof.KALAVATHY PONNIRAIVAN, M.D.**, DEAN., Madras Medical College for giving me permission to conduct the study in this institution.

With extreme gratefulness, I express my indebtness to **Prof.T.S.SWAMINATHAN, MDRD, DMRD, FICR,** Director, Barnard Institute of Radiology, for having encouraged me to take up this study .But for his guiding spirit, perseverance and wisdom, this study would not have materialized.

I express my sincere thanks and gratitude to my guide **Prof. V.CHANDRASEKAR, MDRD, DMRD,** Head of the Department, Barnard Institute of Radiology, for his immense kindness, constant support and consistent encouragement in conducting this study.

I wish to thank **Prof.KUPPUSWAMY, MDRD, DMRD, Prof.N.KULASEKARAN, MDRD, DMRD, Prof.C.ANNADURAI, MDRD,DMRD, Prof.K.VANITHA, MDRD, DMRD, DRM** for their support, valuable criticism and encouragement

I am greatly indebted to my Assistant professors **Dr. UMAPATHY, DMRD, Dr.SUNDARESWARAN, DMRD, Dr.NESAM MANIVANNAN DMRD, Dr.R.RAVI, MDRD, Dr.BABU PETER MDRD, Dr.RAMESH MDRD** and **Dr.C.AMARNATH, MDRD** for their untiring help.

I thank my fellow postgraduate colleagues for their help and co-operation during the study.

I thank all the staff of BARNARD INSTITUTE OF RADIOLOGY for helping me in conducting this study

I thank my parents and my wife for their support and encouragement. Finally I thank all my patients for their cooperation without whom this study would not have materialized.

CONTENTS

INTRODUCTION

Brain tumours are among the common neoplasms of humans. Patients tend to concentrate in institutions where diagnostic and the therapeutic services are available. The incidence of brain tumors is around 4 per 1,00,000 population. Supratentorial brain tumours constitute about 80% of brain tumours in adults and 40% of tumours in paediatric population. Brain neoplasms are found in 2% of autopsy series and account for 1% of all the hospital admissions[1].

Diagnosis of brain tumours may be delayed as the initial symptoms and signs are vague and nonspecific. The symptoms include headache, focal seizures and focal neurological deficit, with clinical examination revealing, raised intracranial tension or focal neurological deficit.

Therefore the clinicians rely heavily on imaging for an early and accurate diagnosis. Significant advance has been made during the last two decades in radiological diagnosis and characterization of brain neoplasms.

The goals of diagnostic imaging in the patient with suspected intracranial tumor include detection of the presence of a neoplasm, localization of the extent of the tumor (including definition of involvement of key structures and assessment of the presence and severity of secondary changes, e.g., edema, herniation, hemorrhage), and characterization of the nature of the process.This has been made possible by modern imaging

modalities like CT and MRI and refinements of previous technique such as angiography. In addition stereotactic biopsy under imaging guidance permits histological diagnosis of brain neoplasm[2].

Both CT and MRI provide excellent anatomic details and information regarding the presence, location and extent of brain tumours.

COMPUTED TOMOGRAPHY:

CT has the capacity to differentiate a wide range of tissue types including air, fat, soft tissue and bone with superior spatial resolution. The use of iodinated contrast agents allow better delineation of vascular anatomy and pathological entities, and can differentiate enhancing lesion from surrounding reactive change. CT is highly sensitive to calcification and blood within the brain parenchyma. CT is preferred for the uncooperative and unstable patients, because each axial image is obtained separately. Thus, motion artifact is minimized, particularly in later generation scanners which can perform individual scans in less than 2 seconds.

CT characterization provides a better insight to the nature of lesion and its effect on the adjacent structures. It also provides a road map for the neurosurgeon regarding the approach, likely duration of surgery, requirements for anaesthesia etc.

Upgradation in recent CT technologies like helical mode helps in 3 dimensional visualization of the neoplasm.

Wider experience in CT and familiarity of the lesions in CT favor CT as an important and appropriate investigation tool.

MAGNETIC RESONANCE IMAGING:

MRI has rapidly earned recognition as the optimal screening technique for the detection of most intracranial neoplasms. Compared with CT, MRI using spin echo, gradient echo, and combination spin and gradient echo pulsing sequences before and after intravenous (IV) administration of paramagnetic contrast agents provides inherently greater contrast resolution between structural abnormalities and adjacent brain parenchyma and has proved to be even more sensitive in the detection of focal lesions of the brain. Early experience suggested that upto 30% more focal intracranial lesions could be identified on MRI than on CT[3,4].

AIMS OF THE STUDY

To assess the role of computed tomography, magnetic resonance imaging in

1) Detection & localization of primary brain tumours.

2) Characterisation of lesions, assessing extent and mass effect of lesions.

3) Giving specific diagnosis of the tumours using characteristics shown by CT and MRI.

REVIEW OF LITERATURE

HISTORY:

Within years after Wilhelm C. Roentgen announced the discovery of x-rays in 1895, Church reported the first use of x-rays to localize a brain tumour, a densely calcified cerebellar tumour. It soon became evident, however, that a non calcified lesion would be virtually indistinguishable by plain film alone.

The introduction of air ventriculography and pneumo encephalography by Walter Dandy in 1918 made it possible to deduce by indirect means the presence and size of intracranial masses by their compressive effect on the air filled ventricular system.

In 1927, Egas Moniz introduced cerebral angiography in which iodinated positive contrast was instilled into the intracranial arterial system; This allows for a more accurate diagnosis of intracranial masses by analysis of displacement of cerebral vessels.

For more than 50 years, pneumoencephalography and cerebral angiography were the only modalities for neuroradiological diagnosis of brain tumours.

With the advent of computer tomography in 1972 by Hounsfield, a British Physicist, cross sectional imaging techniques have since replaced these techniques for the evaluation of intracranial mass lesion. The original

EMI scanner was designed specifically for evaluation of the brain. In this unit the head was enclosed in a water bath between the x-ray to be above and a pair of detectors below.

One major objective of the later second and third generation scanners was to shorten the scanning time for each tomographic section.

Recently developed CT technology, spiral CT permits rapid volume data acquisition and reconstruction of the image in any plane. These techniques are faster than conventional CT and so there is less likelihood of motion artifacts.

The phenomenon of Magnetic resonance was described independently but almost simultaneously by Bloch and Purcell and their colleagues in 1946.Human in vivo images were first published in 1977 by Mansfield & Maudsley, Damadian et al and Hinshaw et al. Hawkes et al in 1980 demonstrated the multiplanar facility of MRI and reported the first demonstration of intra cranial pathology using MR.

DIAGNOSTIC IMAGING

Computed Tomography (CT)

Before the introduction of computed tomography (CT) in the early l970s, confirmation of the presence or absence of brain tumor involved the use of invasive diagnostic procedures (e.g., cerebral angiography or pneumoencephalography) that required hospitalization and carried some

morbidity and risk. Clinicians were often reluctant to submit patients with uncertain history and findings to such risks.

The advent of CT significantly altered the method and timing of diagnostic evaluation of the patient with suspected brain tumor.[5, 6] CT evaluation of the brain is relatively noninvasive and is therefore easily and rapidly accomplished. In the mid-1970s, CT emerged as the primary diagnostic screening modality for the detection of intracranial disease. Areas of structural abnormality (e.g., tumors) appeared on CT as regions of altered tissue radiographic density. Accuracy of localization with CT exceeded the accuracy that could be achieved by cerebral angiography or other invasive diagnostic procedures. Another important advantage of CT was the demonstration of no disease in the symptomatic patient who did not have a neoplasm or other structural abnormality, thus affording reassurance to the patient and physician and avoiding costly hospitalization and more invasive or more hazardous diagnostic procedures.[7] Conversely, CT occasionally revealed abnormalities (including tumors) that were not suspected clinically in patients with relatively nonspecific complaints.

Magnetic Resonance Imaging (MRI)

Lesions and tissues with increased water content appear even more conspicuous on T2-weighted MR images than on CT images obtained after IV infusion of contrast agents[8]. Delineation by MRI of normal and abnormal soft tissue anatomy in the posterior cranial fossa, near the base of the skull,

and in other areas of the brain that lie adjacent to dense bone is considerably better than with CT because of MRI's lack of the beam hardening artifacts secondary to absorption of x-rays in bone seen on CT. Accuracy of lesion localization on MRI is enhanced by its direct multiplanar capability, which permits acquisition of images in the coronal and sagittal plane in addition to the axial plane conventionally used in CT. MRI offers superior contrast resolution, including greater sensitivity for the detection of subacute and chronic hemorrhage in association with tumors and other structural lesions of the brain.

The ability with MRI (using conventional anatomic imaging protocols as well as MRI angiography sequences that display blood flow) to visualize vessels supplying and draining structural lesions in the brain adds yet another important dimension of information that can contribute to the diagnostic assessment.

Even with current state of the art equipment utilizing very high magnetic fields and rapidly switching gradient coils, MR nevertheless suffers two disadvantages in comparison with CT in the assessment of intracranial structural abnormalities. 1.MRI requires significantly longer acquisition times and 2. Abnormalities involving cortical bone, intratumoral calcification, and hyperacute hemorrhage are more clearly and accurately assessed with CT. Newer multi-slice helical or spiral CT scanners are capable of providing highly collimated submillimeter thickness sectional

images in extremely short acquisition times, and thus areas of hyperostosis or bone destruction, intratumoral calcifications, and early intratumoral or peritumoral hemorrhage are more completely defined with greater certainty on CT than on MRI. The much faster acquisition capability of current CT units strongly favors their use in patients who are critically ill or medically unstable. Also, in patients with magnetically controlled cardiac pacemakers and other internal paramagnetic metallic devices, the risk of the MRI magnet interacting with such devices may preclude the use of MRI.

Given both the higher cost and more restricted availability of MR equipment to date as well as continuing improvements in CT equipment and scanning techniques that permit shorter examination times with improved spatial and contrast resolution, it is not surprising that CT remains a major imaging technique for the follow up of intracranial mass lesions. In current clinical practice initial diagnosis and localization of brain lesions are most often accomplished with MRI, but the imaging modality of convenience for followup studies is often CT.

Multiplanar MRI also increases the diagnostic precision with which paraventricular masses can be differentiated from intraventricular masses. Paraventricular tumour characteristic all displace the choroid plexus and compress the lateral ventricles, whereas intraventricular masses cause local ventricular expansion and, generally conform to the shape of the ventricle.

Imaging (usually magnetic resonance imaging (MRI) is extensively utilized in treatment planning before surgery or radiation to define the gross tumour margins and to permit selection of the safest approach to the lesion.

Functional MRI is increasingly employed preoperatively to determine the location of functionally eloquent cortex, which can then be avoided during an operative approach. Interactive computerized neuronavigational devices utilize these data (1) to allow administration of very high doses of precisely focused radiation to small (up to 3 cm) intracranial tumors while sparing the adjacent normal brain and (2) to accurately register the previously acquired image data set onto intraoperative space, thus enabling precise intraoperative localization of surgical instrumentation relative to tumor margins, key vascular structures, and other critical anatomy. A relatively new and highly promising application is image guided surgery, in which the entire surgical resection is guided by direct real time MRI in the operating room environment.

Follow up assessment of intracranial neoplasms utilizes CT and MRI and related techniques extensively, including MRI spectroscopy and MRI perfusion weighted imaging, to monitor post-treatment complications and to detect the presence of residual or recurrent tumor.

NEWER DIAGNOSTIC TECHNIQUES:

Accumulated experience together with continuing improvements in contrast discrimination and spatial resolution have permitted highly accurate correlation between CT and MRI appearance and histologic grading of supratentorial gliomas. However noninvasive differentiation between high grade glioma with a cystic or necrotic center, solitary metastatic carcinoma with central necrosis, resolving hematoma, resolving infarction, atypical mass like presentation of a tumefactive multiple sclerosis plaque, and cerebral abscess on the basis of CT or MRI findings remains a difficult task. Also, precise and accurate separation of infiltrating high grade glioma from surrounding edema is not currently attainable with either conventional MRI or CT, even after IV administration of contrast medium. Differentiation between recurrent tumor and radiation necrosis is another major diagnostic problem in the management of the patient with malignant glioma who has already undergone surgical resection with postoperative radiation therapy. Newer diagnostic techniques based on magnetic resonance are addressing these problems.

Magnetic Resonance Spectroscopy (MRS)

In magnetic resonance spectroscopy (MRS), the resonance signal that is utilized to generate an image in MRI is instead used to generate a frequency spectrum reflecting the components that make up that image[9]. In normal brain tissue, these components reflect both the water content of the brain and the metabolism of the normal neurons and glial cells. If the signal

from water is suppressed, the frequency spectrum (expressed in parts per million [ppm]) reflects the cellular metabolism of the brain in the voxel or section of tissue being interrogated.

The highest- peak amplitude in the normal brain frequency spectrum is that of N-acetyl aspartate (NAA), which occurs at a frequency of 2.0 ppm. NAA is a specific marker of neuronal density and viability. The next highest peak in the normal brain spectrum is that of creatine (Cr), at 3.03 ppm; creatine is involved in energy dependent processes of cellular metabolism in many different types of cells. The third highest peak of the normal brain spectrum is that of choline (Cho), which is involved in and reflects the metabolism of cellular membrane turnover; its frequency peak is 3.2 ppm. In normal brain, the ratio of the height of the choline peak to that of the creatine peak (Cho/Cr) is less than 1.0.

Another important metabolite peak occurs at approximately 1.32 ppm and reflects both lipids and lactate. Lactate is not a normal constituent of brain metabolism; its presence indicates that the normal cellular oxidative metabolism has been altered and that glycolysis is taking place via anaerobic pathways. An elevated lactate peak is seen in the presence of cellular necrosis and reflects lesions that have outgrown their blood supply- for example, the central portions of abscesses, malignant gliomas, lymphomas, and carcinomatous metastases. Lipids resonate at a similar frequency and are also found in highly malignant tumors.

When the interrogating voxel is placed on the peripheral contrast enhancing rim of a rounded intracerebral mass with central hypointensity on TI -weighted MRI, the MR spectroscopic pattern demonstrating elevation of the choline peak with depression of the NAA and creatine peaks is typical for both primary and secondary malignant tumors of the brain and does not aid in their differentiation. MRS of the central hypointense region of such a mass demonstrates elevated lactate and lipid signals, which indicate only the presence of necrosis and do not provide differential information. However, the choline peak in peripheral viable tissue is not elevated in inflammatory processes such as fungal, parasitic, and bacterial abscesses, possibly representing an important differential finding[10].

It is clearly established that in malignant gliomas, infiltrating tumor cells are present well beyond, the contrast enhancing tumor margins seen on CT scans and MR images. However, in metastasis, the peritumoral region contains no infiltrating tumor cells. Studies involving MR spectroscopic interrogation of the peritumoral region in patients with solitary brain tumors have document elevated choline levels with reversal of the normal Cho/Cr ratio in the peritumoral region in patients who have infiltrating high grade gliomas but not in patients who have metastases[11]. This finding on MRS may enable the discrimination between malignant glioma and metastasis and suggests that the peritumoral hyperintensity on T2-weighted images and the peritumoral hypointensity on T1- weighted images seen in association with malignant gliomas may reflect not only

vasogenic edema but also tumor infiltration, whereas the lack of reversal of the normal Cho/Cr ratio in the peritumoral tissue surrounding metastases suggests that the similar MRI appearance of this tissue is likely due to edema or gliosis.

PERFUSION-WEIGHTED MRI

Another difference between patients with malignant glioma and those with metastasis has been noted on dynamic contrast enhanced perfusion-weighted MRI utilizing a first pass image acquisition protocol after bolus IV administration of gadolinium[12]. One Study has demonstrated a significant increase in relative cerebral volume (rCBV) in the peritumoral region in patients with malignant gliomas, and a diminished rCBV in the peritumoral region in patients with metastases. Increased peritumoral perfusion in patients with malignant gliomas is presumed to be due to tumor infiltration into the peritumoral region with associated loss of blood-brain barrier integrity. Diminished peritumoral perfusion in the tissue surrounding a metastasis may reflect an intact blood-brain barrier with the vasogenic edema causing local compression of the microcirculation.

POSITRON EMISSION TOMOGRAPHY

Studies of cerebral oxygen metabolism using the positron-emitting isotope fluorine- 18 tagged 2 fluoro deoxyglucose **(**FDG), an analogue of glucose, have established that most malignant brain tumors have increased glucose uptake and metabolism compared with normal brain parenchyma,

that the level of FDG uptake correlates well with histologic grade in cerebral gliomas, and that FDG positron emission tomography (PET) is a good predictor of prognosis in these tumors[13].

Differentiation between recurrent tumor and radiation necrosis remains a major unsolved problem in the management of patients with malignant gliomas. Both processes can present the heterogeneous appearance of a growing infiltrative mass with irregularly marginated contrast enhancement on CT and MRI. Early work suggested that necrotic tissue failed to take up the radioactivity and appeared hypometabolic and that actively growing tumor demonstrated strong hypermetabolic uptake. This finding was verified on a subsequent study demonstrating high sensitivity and specificity for FDG PET. However, other studies have questioned the accuracy and specificity, and therefore the utility, of FDG PET for this indication.

CLASSIFICATION OF PRIMARY BRAIN TUMOURS

Bailey & Cushing in 1926 were the first to propose classifications of brain tumours based on the cell of origin, subsequently developed by Russel and Rubinstein in 1989, WHO subsequently devised a modification to Russel and Rubinstein classification in 1994 thus giving an impetus and standardization of Brain tumours. Neurons and neural glialcells are the two tissues that make up the central nervous system. Neuroglia consist of Astrocyte,Oligodendrocyte, microglia, ependyma and choroid epithelium.

Vast majority of brain tumours arise from the neuroglia and are included under a broad term gliomas. Added to the list of primary tumours are tumours arising from the pineal Body, meningiomas, germ cell tumours, and lymphoma. Dermoid, epidermoid, arachnoid cyst and colloid cyst are considered to be maldevelopmental in origin. Metastatic tumours represent secondary malignancies of the brain and its coverings.

The current International Histological classification of CNS tumours drafted in 2000 revision by the World Health Organisation is as follows[14].

This classification has been adapted and modified from Kleihues P, Cavenee WK (eds): Pathology and genetics of the tumours of the nervous system. Lyon, international agency for research on cancer ,2000.

GLIAL TUMOURS

Astrocytomas

Circumscribed Astrocytomas

Juvenile Pilocytic Astrocytoma
Pleomorphic Xanthoastrocytoma
Subependymal giant cell astrocytoma

Diffuse Astrocytomas

Low grade astrocytomas

Optic pathway Glioma

Brain stem Glioma

Anaplastic Atrocytoma

Glioblastoma Multiforme

Gliomatosis Cerebri

Gliosarcoma

Oligodendroglioma

Low Grade Oligodendroglioma

Anaplatsic Oligodendroglioma

Ependymomas

Ependymoma

Subependymoma

Choroid plexus tumours

Choroid plexus papilloma

Choroid plexus carcinoma

NONGLIAL TUMOURS

Neuronal and mixed

Neuronal / glial tumours

Ganglioglioma
Gangliocytoma
Lehermitte – Duclos disease
Desmoplastic infantile ganglioglioma
Dysembryoplastic Neuro Epithelial Tumour
Central neurocytoma

Pineal Parenchymal tumours

Pineoblastoma

Pineocytoma

Embryonal tumours

Medulloblastoma

Supratentorial primitive neuroectodermal tumours

TUMOURS OF THE CRANIAL NERVES

Schwannoma

Neurofibroma

Malignant Peripheral nerve sheath tumours

TUMOURS OF THE MENINGES

Meningioma

Hemangiopericytoma

Mesenchymal non meningothelial tumours

Melanocytic tumours

Hemangioblastoma

TUMOUR OF THE HEMOPOIETIC SYSTEM

Primary CNS Lymphoma

Secondary CNS Lymphoma

Histiocytic lesions

Granulocytic sarcoma

GERMCELL TUMOURS

Germinoma

Teratoma

Other germ cell tumours

TUMOURS OF THE SELLAR REGION

Pituitary adenoma

Miroadenoma

Macroadenoma

Craniopharyngioma

Rathke cleft cyst

Tumours Of The Neuro Hypophysis

Chordoma

METASTATIC TUMOURS

Metastases to the brain

Metastases to the skull and intracranial dura

Leptomeningeal Metastasis (leptomeningeal carcinomatosis)

CHARACTERISTICS OF PRIMARY BRAIN TUMOURS

Location:

Tumour location is important for differential diagnosis of brain neoplasms and for determining imaging technique. Coronal plane imaging of the sella is an example of adjusting imaging technique for tumour location[15].

Extra axial location are typical of Benign intracranial neoplasm and parenchymal infiltration is characteristic of malignant brain tumours. On imaging extra axial masses buckles the white matter, expands the ipsilateral subarachnoid spaces, and sometimes causes reactive bone changes. An intraxial mass expands the cortex of the brain, separation of the lesion from the underlying leptomeninges is not seen, lesion spreads across well defined boundaries, and the dura is seen peripheral to the mass.

List of differential diagnosis of common supratentorial primary Brain tumours in relation to the anatomical location.

I. Cerebral Hemispheres
   Astrocytoma
   GBM
   Oligodendroglioma
   Meningioma

II. Leptomeninges & Dura
   Meningioma
   Metastasis
   Lymphoma
   Leukemia

III. Deep structure (periventricular, thalamus and basal ganglia)
   Primary Cerebral lymphoma
   Primary Cerebral neuroblastoma
   Glioma – often High grade

IV. Corpus Callosum

GBM

Lymphoma

Metastasis

Lipoma (in Corpus Callosal Agenesis)

V. Lateral ventricle

Ependymoma

Meningioma

Choriod plexus Papilloma

Primary cerebral neuroblastoma

Subependymoma

VI. Foramen of Monro

Giant cell astrocytoma

Colloid cyst

Ependymoma

Subependymoma

VII. Third Ventricle

Colloid cyst

Ependymoma

VIII. Optic chiasma region

Pilocytic astrocytoma

Craniopharyngioma

Meningioma

Germinoma

Arachnoid cyst

IX. Pituitary region

Adenoma

Craniopharyngioma

Meningioma

Dermoid tumour

Rathke Cleft cyst

X. Pineal region

Germinoma

Teratoma

Pineocytoma

Glioma

INFRATENTORIAL LESIONS

ADULT

Metastases

Hemangioblastoma

Acoustic schwannoma

Meningioma

Epidermoid

Other schwannomas

Vascular lesions

Paragangliomas

CHILDREN

Medulloblastoma

Cerebellar astrocytoma

Brainstem glioma

Ependymoma and choroids plexus papilloma

MARGINS:

Smooth, sharply defined margins favor the diagnosis of benign lesion, and irregular, poorly defined margins favor malignant neoplasms, due to their tendency for parenchymal infiltration.

PARENCHYMA:

Heterogenicity in a tumour are due to Hemorrhage, calcification, fat, cyst formation and necrosis.

CT & MRI CHARACTERISTICS OF COMMON PRIMARY NEOPLASMS[16]

1. DIFFUSE ASTROCYTOMA, LOW GRADE

CT Findings

NECT

- Illdefined homogeneous hypodense/isodense mass
- 20% Ca++; cysts are rare
- Calvarial erosion in cortical masses (rare)

CECT

- No enhancement or very minimal
- Enhancement should raise suspicion of focal malignant degeneration

MR findings

- T1WI
  - Homogeneous hypointense mass
  - May expand white matter and adjacent cortex
  - Appears circumscribed, but infiltrates adjacent brain
  - Hemorrhage or surrounding edema (rare)

- T2WI
    - Homogeneous hyperintense mass
    - May appear circumscribed, but often infiltrates adjacent brain
- FLAIR: Homogeneous hyperintense mass
- DWI: Restricted diffusion usually absent
- T1 C+ :
    - Usually no enhancement
    - Enhancement suggests progression to higher grade
- MRS
    - High choline, low NAA typical but not specific

2. ANAPLASTIC ASTROCYTOMA

CT Findings

NECT

- Low density ill-defined mass
- Ca++ and hemorrhage rare

CECT

- Majority do not enhance
- Enhancement often focal, patchy, heterogeneous

MR findings

- T1WI
    - Mixed isointense to hypointense WM mass
    - Ca++, hemorrhage, cysts rare

- T2WI
  - Heterogeneously hyperintense
  - May appear discrete, but infiltrates adjacent brain
  - May involve and expand overlying cortex
  - Ca++, hemorrhage, cysts are rare
- FLAIR: Heterogeneously hyperintense
- DWI: No diffusion restriction is typical
- T1 C+ :
  - Usually no enhancement
  - Less common: focal, nodular, homogeneous, patchy enhancement

3. GLIOBLASTOMA MULTIFORME

CT Findings

NECT

- Irregular isodense or hypodense mass with central hypodensity representing necrosis
- Marked mass effect and surrounding edema/tumour infiltration
- Hemorrhage not uncommon
- Ca++ rare (related to low grade tumor degeneration)

CECT: 95% have strong, heterogeneous, irregular rim-enhancement.

MR findings

- T1WI
  - Irregular isointense, hypointense white matter mass
  - Necrosis, cysts and thick irregular margin common may have sub acute hemorrhage.

  T2WI :

  - Hetegeneous, hyperintense mass with adjacent tumor infiltration/ vasogenenic edema.
  - Viable tumor extends far beyond signal changes

  Necrosis, cysts, hemorrhage, fluid/debris levels, flow voids (neovascularity) may be seen

  - FLAIR: Heterogeneous, hyperintense mass
- DWI :
  - Lower measured ADC than low grade gliomas
- T1 C+ :
  - Thick, irregular rind of enhancement surrounding central necrosis typical
  - Enhancement may be solid, ring, nodular or patchy

4. PILOCYTIC ASTROCYTOMA

CT Findings

NECT

- Discrete cystic/solid mass
- May have little or no surrounding edema
- Ca++, 20%, hemorrhage rare

CECT

- >95% enhance (pattern vary)
- 50% nonenhancing cyst, strongly enhancing mural nodule.

MR findings

- T1WI
  - Solid portion iso/hypointense to GM
  - Cyst contents iso-to slightly hyperintense to CSF
- T2WI
  - Solid portions hyperintense to GM
  - Cyst contents hyperintense to CSF
- FLAIR:
  - Solid portions hyperintense to GM
  - Cyst contents do not suppress: Hyperintense to CSF
- T1 C+:
  - Intense but heterogeneous enhancement of solid portion
  - Cyst wall occasionally enhances

5. PLEOMORPHIC XANTHOASTROCYTOMA

CT Findings

NECT

- Cystic/Solid mass: Hypodense with mixed density nodule
- Minimal or no edema is typical
- Ca++, hemorrhage, frank skull erosion rare

CECT: Strong, sometimes heterogeneous enhancement of tumor nodule.

MR findings

- T1WI
  - Mass is hypointense or isointense to gray matter
  - Mixed signal intensity may be seen
  - Cystic portion isointense to CSF
- T2WI
  - Hyperintense or mixed signal intensity mass
  - Cystic portion isointense to CSF
- FLAIR: Hyperintense or mixed signal intensity mass
- Cystic portion isointense to CSF
- T1 C+ :
  - Enhancement usually moderate/strong, well-delineated
  - Enhancement of adjacent meninges, dural "tail" common approximately 70 %.
  - Enhancing nodule often abuts pial surface

6. SUBEPENDYMAL GIANT CELL ASTROCYTOMA

CT Findings

NECT

- Hypodense → Isodense
- Ca++ variable
- Hydrocephalus

CECT

- Heterogeneous, strong enhancement
- Initially tumor typically >1cm

MR findings

- T1WI
  - Hypointense to isointense to GM
  - ±Ca++ (hyperintense to hypointense)
- T2WI
  - Heterogeneous
- FLAIR: Heterogeneous hyperintense
- Periventricular interstitial edema from ventricular obstruction

7. OLIGODENDROGLIOMA

CT Findings

NECT

- Mixed density(hypodense/isodense) hemispheric mass that extends to cortex.
- Majority calcify, nodular or clumped Ca++ (70-90%)
- Cystic degeneration common (20%)

CECT

- Approximately 50% enhance
- Enhancement varies from none to striking

MR findings

- T1WI
  - Hemispheric mass, hypointense to isointense to GM
  - Typically heterogeneous
  - Cortical and subcortical with cortical expansion
- T2WI
  - Typically heterogeneous, hyperintense mass
  - Heterogeneity related to Ca++, cystic change, blood products
- Typically expands overlying cortex
- FLAIR
  - Typically heterogeneous, hyperintense
- DWI: No diffusion restriction is typical
- T1 C+ :
  - Heterogeneous enhancement is typical

8. EPENDYMOMA

CT Findings

NECT

- Infratentorial
  - 4th ventricular tumour extends into CPA/Cisterna magna
  - Ca++ common (50%); +/- cysts, hemorrhage
- Supratentorial
  - Large heterogeneous periventricular mass
  - CA++ common (50%)

CECT: Variable heterogeneous enhancement

MR findings

- T1WI
  - Heterogeneous, usually iso-to hypointense
- T2WI
  - Heterogeneous, usually iso-to hyperintense
- FLAIR
  - Can show sharp interface between tumour and CSF
  - T1 C+: Mild to moderate, hetetogeneous enhancement

9. SUBEPENDYMOMA

CT Findings

NECT

- Isodense to hypodense intraventricular mass
- Cysts or Ca++ may be seen in larger lesions.

CECT

- No enhancement, mild enhancement typical

MR findings

- T1WI
  - Intraventricular mass, hypointense or isointense to white matter
  - Typically homogeneous solid mass
- T2WI
  - Hyperintense intraventricular mass

- FLAIR: Hyperintense intraventricular mass
- T1 C+: Variable enhancement, typical none to mild

10. CHOROID PLEXUS PAPILLOMA

CT Findings

NECT

- Intraventricular bosselated mass
- 75% iso-or hyperattenuating
- Ca++ in 25%, hydrocephalus

CECT

- Intense, homogeneous enhancement
- Heterogeneous enhancement suggests choroid plexus carcinoma (CPCA)

MR findings

- T1WI
  - Well delineated, lobulated mass
  - Iso-to hypointense
- T2WI
  - Iso-to hyperintense
- FLAIR: Bright periventricular signal
- T1 C+ : Robust homogeneous enhancement
- MRA: Flow related signal within mass
- Enlarged choroidal artery (trigonal mass)

11. DYSEMBRYOPLASTIC NEURO EPITHELIAL TUMOUR-DNET

CT Findings

NECT

- Wedge-shaped low density area
- Cortical / subcortical lesion
- Scalloped inner table in 44-60%.

CECT

- Usually nonenhancing

MR findings

- T1WI
  - Pseudocystic, multinodular ("bubbly") mass
  - Hypointense on T1
- T2WI
  - Very hyperintense on T2
- FLAIR: Mixed (hypo/isointense) signal with "bright" rim.
- DWI: Usually lacks restricted diffusion
- T1 C+: Usually does not enhance

12. CENTRAL NEUROCYTOMA

CT Findings

NECT

- Usually mixed solid and cystic (Isodense/hyperdense)
- Ca++ common, 50-70%
- Hydrocephalus common

CECT: Moderate, heterogeneous enhancement

MR findings

- T1WI
  - Heterogeneous, mostly isointense to gray matter cysts are hypointense.
- T2WI
  - Heterogeneous, hyperintense "bubbly" appearance
- FLAIR: Heterogenous, predominantly hyperintense mass
- T1 C+: Moderate to strong heterogeneous enhancement

13. PINEOBLASTOMA

Imaging Findings

- Large, heterogeneous pineal mass with "exploded", peripheral Ca++
- Nearly 100% with obstructive hydrocephalus

14.PINEOCYTOMA

Imaging Findings

- Enhancing, circumscribed pineal mass which "explodes" pineal ca++
- May mimic pineal cyst or pineoblastoma

15. MEDULLOBLASTOMA (PNET-MB)

CT Findings

NECT

- Solid mass in 4th ventricle
- 90% hyperdense
- Ca++ in upto 20%; hemorrhage rare
- Hydrocephalus common (95%)

CECT

- >90% enhance
- Relatively homogeneous

MR Findings

- T1WI: Hypointense to gray matter (GM)
- T2WI: Near GM intensity
- Flair: Hyperintense to brain
- DWI: Restricted diffusion +
- T1 C+
  - >90% enhance
  - Often heterogeneous

16. SCHWANNOMA

CT Findings

NECT

- Cranial nerve schwannoma
- Noncalcified extra-axial mass
- Iso/slightly hyperdense compared to brain
- May enlarge bony foramina (IAC, foramen ovale, facial nerve canal)

CECT: Strong, uniform enhancement

MR Findings

- T1W1: Usually iso-, sometimes mixed iso-/hypointense
- T2WI: Hyperintense (nodule may be isointense)
- DWI: Solid portion of schwannomas shows no restriction
- T1 C+
    - Enhances strongly
    - Cranial nerve schwannoma: 2/3 solid; 2/3 ring or inhomogeneous.

17. PITUITARY MACROADENOMA

CT Findings

NECT

- Variable attenuation
- Typical - usually isodense with gray matter GM
- Cyst formation , necrosis common
- Hemorrhage 10% ; Ca^{++} 1-2%
- Large Adenomas expand sella, may erode floor
- Aggressive adenomas extend inferiorly invade sphenoid,
- May destroy upper clivus

CECT : Moderate , some what inhomogenous enhancement

MR Findings

T1WI :

- Usually isointense with GM
- subacute hemorrhage has short T1

- Fluid-fluid levels may occur especially with pituitary apoplexy
- PPBS absent in 20 % of large adenomas
- Cavernous sinus invasion difficult to determine (medial wall is thin, weak)

T2WI:

- Most common - isointense with gray matter
- Less common
  - Cysts – hyperintense, hemorrhage
  - Dense granulated GH producing adenomas are often hypointense
  - Uncommon – High signal along optic tracts
  - FLAIR :Hyper intense to brain gray matter
  - T1 C+ : Enhances well
  - MRA : ICA s often displaced, encased rarely occluded.

18. CRANIO PHARYNGIOMA:

CT Findings

NECT

- Adamantinomatous type 90%, mixed solid (iso), cystic (hypodense)
- 90% calcify

CECT: 90 % ENHANCE

MR Findings

- T1 WI :
  - Adamantinous type - hyperintense
  - Papillary type - isointense

- T2WI :
  - Cyst – hyper intense
  - Solid – Hetero intense
- FLAIR : Cyst- Hyperintense
- DWI : Variable
- T1C+: Cyst walls Enhance , solid portions – Heterogenous Enhancement

19. MENINGIOMAS:

CT Findings

NECT:

- Hyperdense 75 %
- Calcification 20% - 25%
- Necrosis rare
- Hyper ostosis and irregular cortex +

CECT :

- More than 90% Enhance homogenously and intensely

MR Findings

- T1 WI : Iso to hypo with GM
- T2WI : Variable
  - Best to visualize CSF cleft
- DWI : Variable
- T1 C+: More than 95% Enhance homogenously and intensely
- Dural tail 35%- 80% of the cases(non specific)

20. ARACHNOID CYST:

CT Findings

NECT: CSF density

CECT : No enhancement

MR Findings

- T1 WI : Isointense to CSF
- T2 WI : Isointense To CSF
- FLAIR : Suppresses completely
- DWI : No restriction
- T1C+ : No enhancement

21. EPIDERMOID CYST :

CT Findings

NECT:

- CSF density
- 10%-25% Calcification +

CECT: May show cyst margin enhancement

MR Findings

- T1WI : Slightly hyperintense to CSF
- T2 WI : Iso intense To CSF
- FLAIR : Not Suppressed completely
- DWI : Restricted diffusion +
- T1C+ : May show cyst margin enhancement (35%)

22. BRAIN STEM GLIOMA:

- Classic Imaging apperance varies with tumour type and location
- TECTAL: Pilocytic, focal, variable enhancement, ca++
- FOCAL TEGMENTAL MESENCEPHALIC: Pilocytic, cyst + nodule
- DIFFUSE PONTINE GLIOMA: Fibrillary, diffuse, non enhancing.

Incidence:

Incidence of intracranial tumours in Indian series by Dr.B.Ramamurthy 1978 to 1994[17].

S.NO	***TUMOURS***	***PERCENTAGE***
1	Gliomas	42.09%
2	Meningiomas	15.09%
3	Pituitary tumours	15.15%
4	Schwannoma	8.99%
5	Metastasis	6.21%
6	Vasoformative tumours	3.37%
7	Developmental tumours	6.42%
8	Lymphoreticulosis	0.58%
9	Skull tumours	0.32%
10	Sarcomas	0.85%

MATERIALS AND METHODS

The study comprised of 80 patients including 41 males and 39 females age ranging from 1 year to 65 years. The study was conducted for a period of 18 months from March 2005 to august 2006.

The patients were referred from Institute of Neurology, Government General Hospital, Chennai, Institute of Child Health, Egmore, Chennai-8 to Barnard Institute of Radiology for radiological evaluation.

Clinically the most frequent symptom was head ache. Predominant clinical features were seizure, focal neurological deficit, cranial nerve palsies and loss of consciousness.

Inclusion Criteria:

All the patients who had radiological features suggestive of primary brain tumour.

Exclusion Criteria:

1) Patients who had already been worked up elsewhere and referred here with tissue diagnosis.

2) Patients with known primary tumor elsewhere in the body with features of metastases to brain.

3) Patients who were contraindicated for magnetic resonance imaging (Pace Makers, Claustrophobia).

COMPUTED TOMOGRAPHY:

CT was done with TOSHIBA X SPEED Third Generation Scanner Machine Parameters:

Tube Voltage : 120 kv

Tube Current : 80 mA

Scanning time : 4 sec

Filter : FC 20

TECHNIQUE OF THE STUDY:

Axial study was performed in all the cases and coronal study was performed in relevant cases especially tumours of sella.

Axial study done with following parameters:

Patient position: Supine with closed Eyes

Slice Thickness : 10 mm

Slice Interval : 10 mm (for supratentorial)

5mm (for infra tentorial)

Plane of Section: Osteo-Meatal Line

Extent of Study: From Base of the Skull to the High parietal region

Protocol For Coronal study:

Patient position: Prone with extended neck and closed Eyes

Slice Thickness : 5 mm

Slice Interval : 5 mm

Plane of Section: Perpendicular to the Hard palate

Extent Of Study: In the region of interest

2mm thin sections were carried out in both axial and coronal studies in the region of interest for better spatial resolution.

Contrast Study was performed in all cases and injected as rapid bolus. Quantity of the contrast media: 60 ml of Iohexol in rapid bolus.

MRI TECHNIQUES

MRI was performed using 1.5 Tesla superconducting SIEMENS MAGNETOM, symphony using head coil.

POSITION: Patient is placed in supine position in the MRI gantry with head coil positioned.

MRI TECHNIQUES USED:

Multiplanar scout sections were obtained for planning sequences. Imaging of whole brain MR from vertex to foramen magnum including base of skull using axial, coronal and saggital sections with the following sequences was done.

T1WI		***T2WI***	
TR: 500 msec	S/G – 5 / 1.5	TR: 4000 msec	S/G – 5 / 1.5
TE: 14 msec		TE: 93msec	
FLAIR		***DWI***	
TR: 9000 msec	S/G – 5 / 1.5	TR: 4300 msec	S/G – 5 / 1.5
TE: 105msec		TE: 123msec b : 0,500,1000	

MRA 3D TOF ***MRV 2D T0F***

TR: 839 msec S/G – 5 / 1.5 TR: 30 msec S/G – 5 / 1.5

TE: 6.8 msec TE : 6.5 msec

GRE T2 Axial

TR: 839 msec S/G – 5 / 1.5

TE: 27msec

Contrast study

It was performed in all cases – axial, sagittal, coronal sections using T1WI were taken.

Quantity of contrast: 0.1 mmol/kg of dimeglumine Gadopentitate.

For interpretation the following aspects of brain tumours were studied and analysed in these patients.

1. **Location**
2. **Margins**
   - Ill defined margins
   - Moderately defined margins
   - Well defined margins
3. **CT Characteristics**
   - Density
   - Calcification
   - Hemorrhage

- Mass effect
- Contrast enhancement

4. **MRI Characteristics**

- T1 Signal intensity
- T2 Signal intensity
- FLAIR
- Diffusion
- Mass Effect
- Contrast Enhancement

The contribution of CT and MR towards the above mentioned aspects were analysed for arriving the radiological diagnosis.

Tissue biopsy and surgical exploration with tissue diagnosis were considered to confirm the diagnosis.

RESULTS AND ANALYSIS

TABLE – 1:
DISTRIBUTION OF PRIMARY BRAIN TUMOURS

S.NO	TUMOURS	NO OF CASES
1	Gliomas	42
2	Meningiomas	11
3	Sellar & Supra Sellar lesions	7
4	Medulloblastoma	7
5	Schwannoma	5
6	Arachnoid cyst	2
7	Epidermoid cyst	2
8	Intraventricular tumours	4

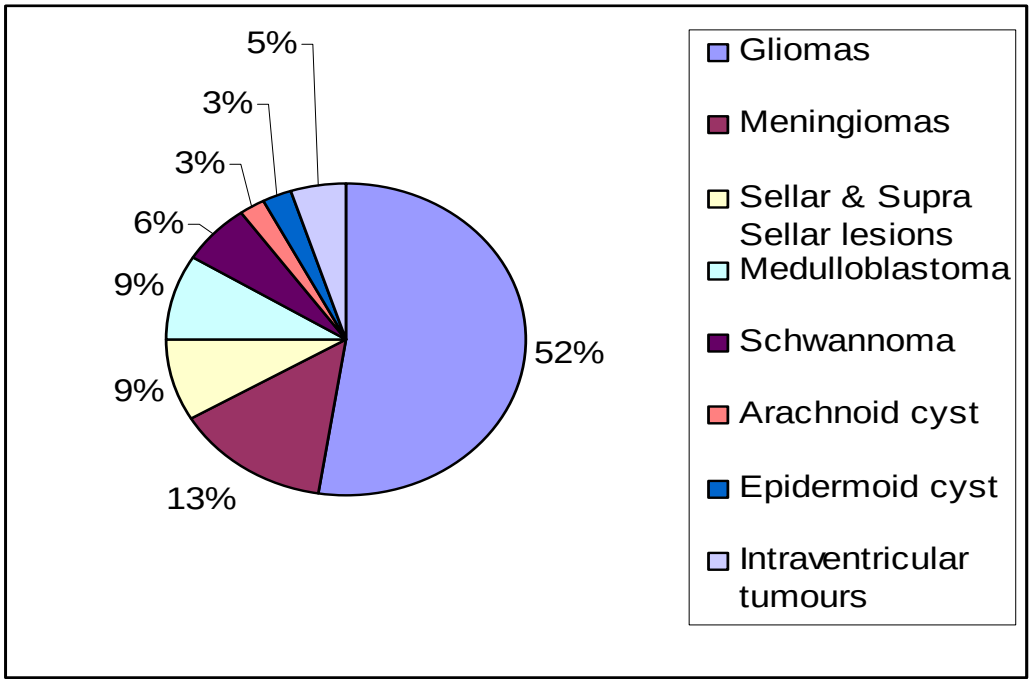

TABLE – 2
SEX DISTRIBUTION

S.NO	TUMOURS	No of cases	sex			
			Male	%	Female	%
1	Gliomas	42	25	59.5	17	40.5
2	Meningiomas	11	3	27.2	8	72.8
3	Sellar & Supra Sellar lesions	7	4	57.1	3	42.9
4	Medulloblastoma	7	4	57.1	3	42.9
5	Schwannoma	5	2	40	3	60
6	Arachnoid cyst	2	0	0	2	100
7	Epidermoid cyst	2	1	50	1	50
8	Intraventricular tumours	4	2	50	2	50

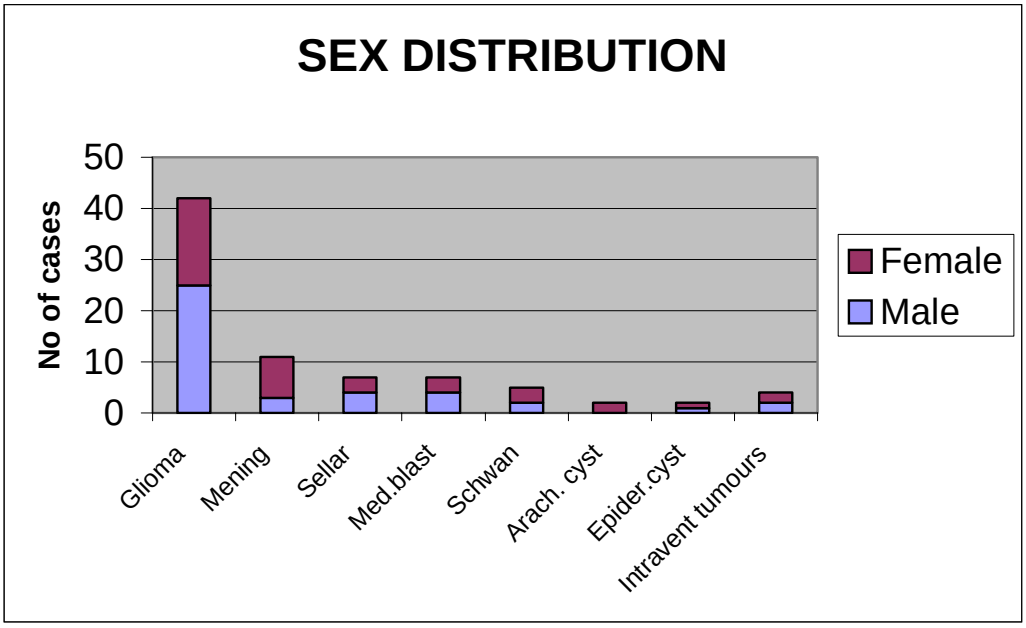

TABLE - 3
AGE DISTRIBUTION

Age	*Glioma*	*Menin-gioma*	*SELLAR*	*Medullo Blastoma*	*Schwa-nnoma*	*Arach cyst*	*Epiderm cyst*	*Intra ventricular*
0-10	1	–	3	3	–	2	–	1
11-20	5	–	1	4	1	–	–	1
21-30	5	2	3	–	–	–	–	2
31-40	7	1	–	–	3	–	1	–
41-50	13	4	–	–	–	–	1	–
51-60	8	3	–	–	1	–	–	–
61-70	3	1	–	–	–	–	–	–

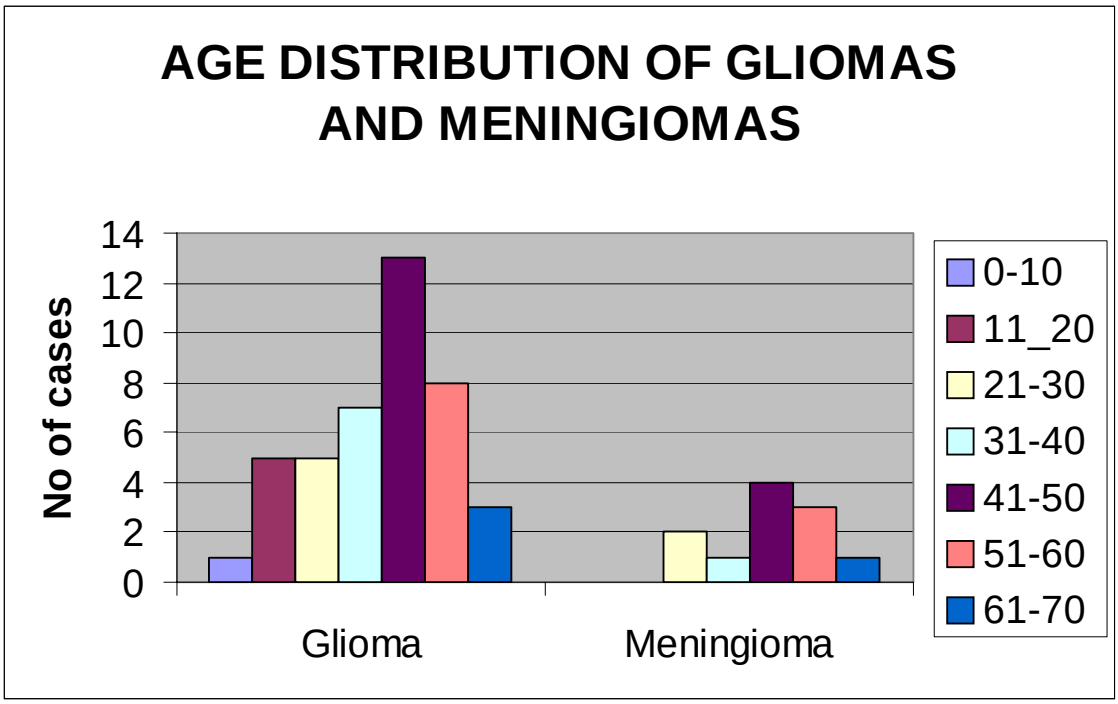

TABLE -4
DISTRIBUTION OF SUB TYPES OF GLIOMAS

S.No	*SUB TYPES*	*No of cases*	*PERCENTAGE*
1	Low grade astrocytoma	8	19.5%
2	Anaplastic astrocytoma	11	26.6%
3	Glioblastoma Multiforme	17	40.9%
4	Circumscribed Astrocytomas	4	9%
5	Oligodendroglioma	2	4%

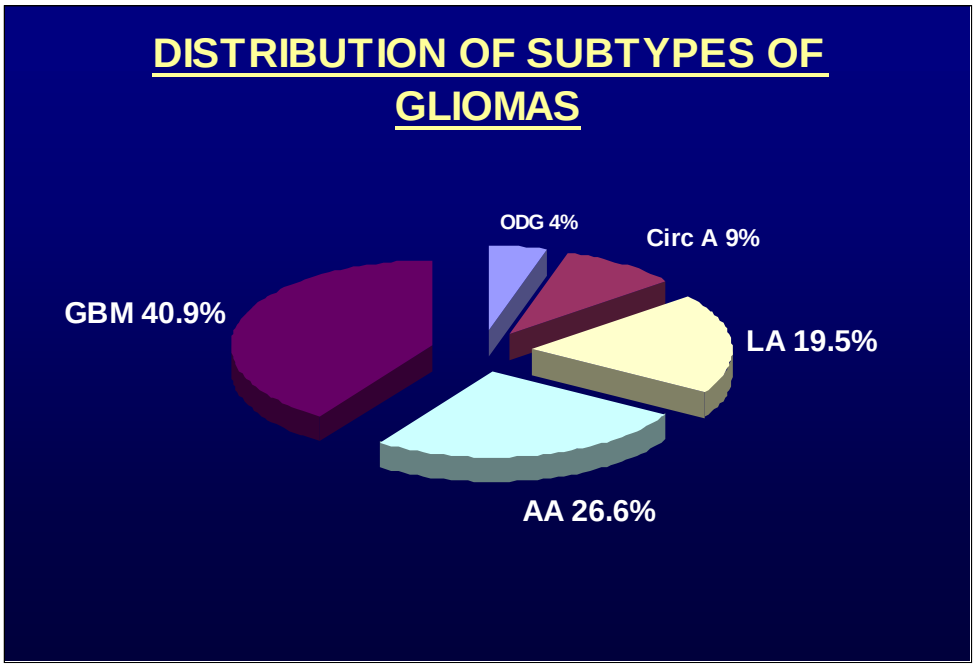

Out of 42 patients of gliomas, 17 patients (40.9%) were GBM, 11 patients (26.6%) were anaplastic astrocytoma.

TABLE – 5
DISTRIBUTION OF PRIMARY BRAIN TUMOURS BY LOCATION

	Distribution	No of cases	Percentage
1.	Supratentorial	59	73.7%
2.	Infratentorial	21	26.3%
	Total	80	-

Most of the primary brain tumours are located supratentorially.

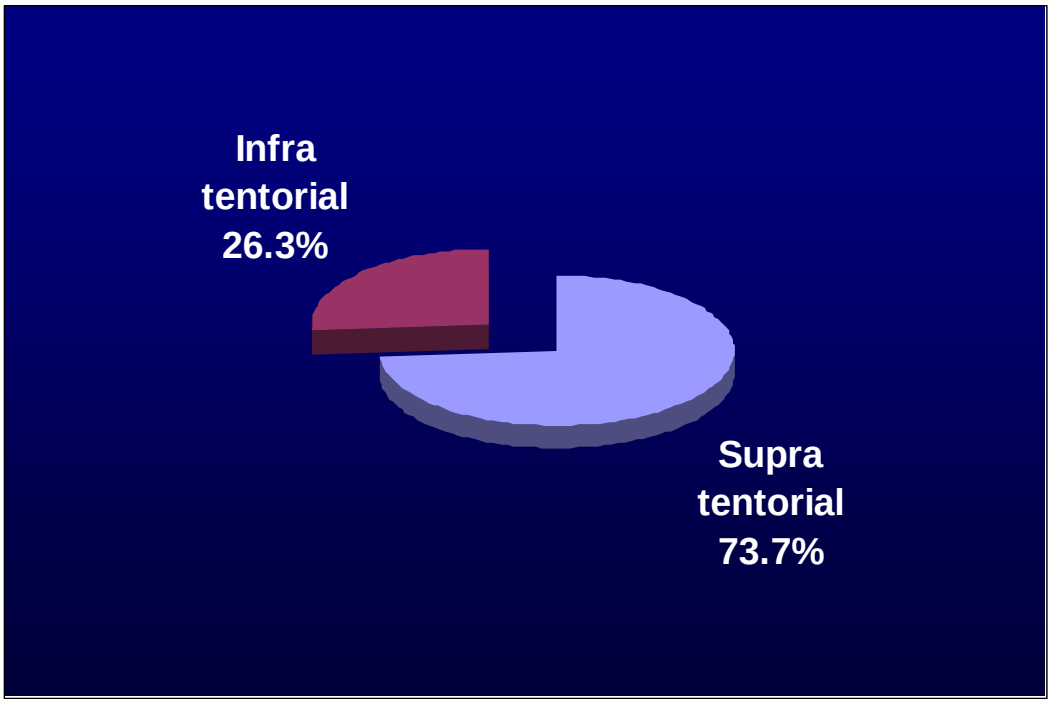

TABLE – 6

		Intraaxial	**%**	***Extra axial***	**%**	***Total***
1.	Supratentorial	37	62.7%	22	37.3%	59
2.	Infratentorial	12	57.1%	9	42.9%	21

Infratentorially the occcurance of extra axial lesion are more common than supra tentorial location(table 5).

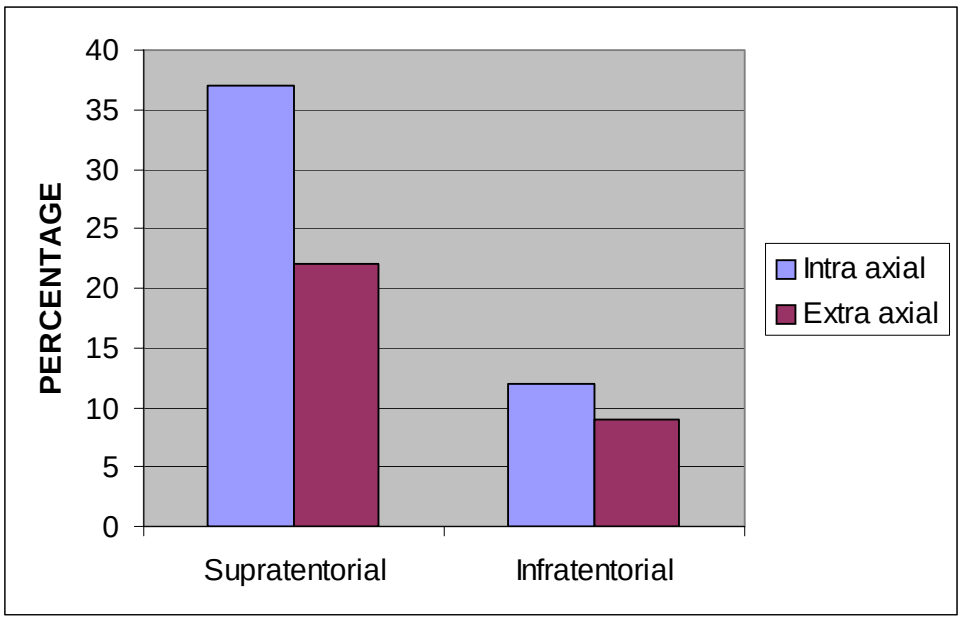

TABLE - 7
INTRAVENTRICULAR TUMOURS

Site	No of cases	%
Body of the lateral ventricles	2	50%
Atrium	1	25%
Foramen of Monro	1	25%

Lateral ventricular tumours were the commonest location for intra ventricular tumours.

TABLE – 8

S.No	***Tumour***	***Total Cases***	***Calcification***		***Hemorrhage***	
			No of cases	***%***	***No of cases***	***%***
1	Glioma	42	5	11.9%	9	21.4%
2	Meningioma	11	3	27.2%	0	-
3	Sellar	7	3	42.8%	0	-
4	Medulloblastoma	7	2	28.5%	0	-
5	Schwannoma	5	0	-	0	-
6	Arachnoid Cyst	2	0	-	0	-
7	Epidermoid cyst	2	0	-	0	-
8	Intraventricular tumours	4	1	25%	0	-

Calcification was noted in 14 cases, out of 80 cases of primary brain tumours.

In glioma of 42 cases only 5 (11.9%) showed calcification. In meningiomas of 11 cases ,3 (27.2%) showed calcification. All 3 cases of craniopharyngioma showed calcification.

Hemorrhage was seen in 9 cases all were proved to be glioblastoma in HPE.

TABLE – 9
MRI SIGNAL CHARACTERISTICS OF TUMOURS

SEQUENCE	HYPO	HYPER	ISO	HET
T1 WI	51	1	4	24
T2 WI	3	37	7	33

Most tumours were hypointense on T1WI and hyperintense on T2 WI.

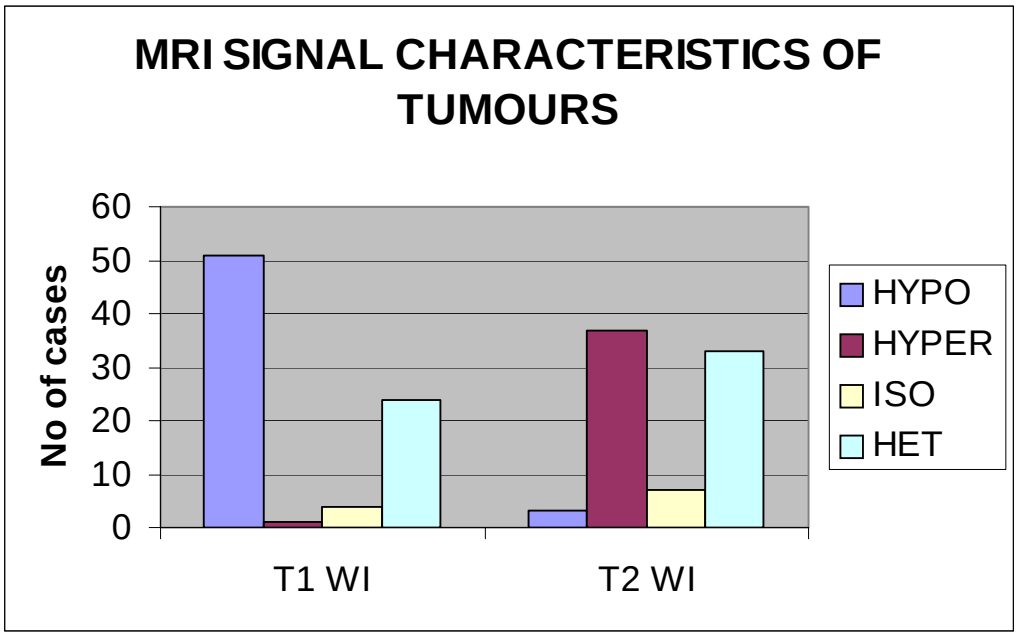

TABLE – 10
CONTRASTENHANCEMENT OF THE GLIOMAS

GLIOMAS	TOTAL	NO CE		ENHANCEMENT			
		No of cases	%	MILD CE	MOD CE	INTENSE	%
LA	8	8	100%	-	-	-	-
AA	11	6	54.5%	3	2	-	45.5%
GBM	17	-	-	-	8	9	100%
CIRC A	4	-	-	2	2	0	100%
ODG	2	-	-	2	-	-	100%

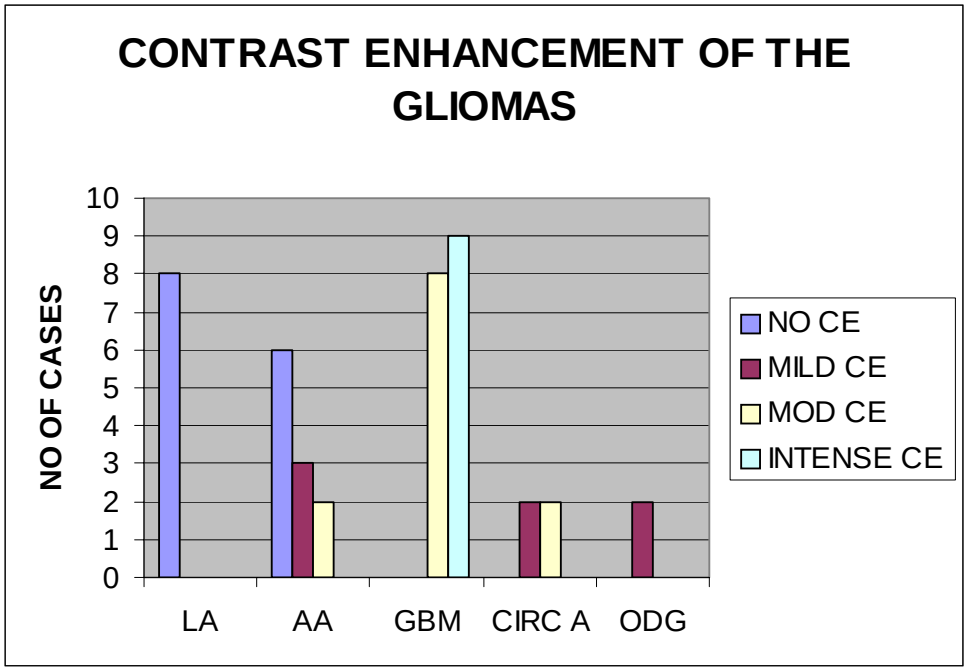

Low grade astrocytoma- No enhancement noted

Mild to moderate enhancement noted in 5 cases(45.5%) of AA.

Moderate to intense enhancement noted in 17 cases (100%) of GBM.

TABLE – 11
MENINGIOMA IN T2WI SEQUENCES

T2	NO OF CASES	PERCENTAGE
ISO	6	55%
HYPO	1	9%
HYPER	2	18%
HET	2	18%

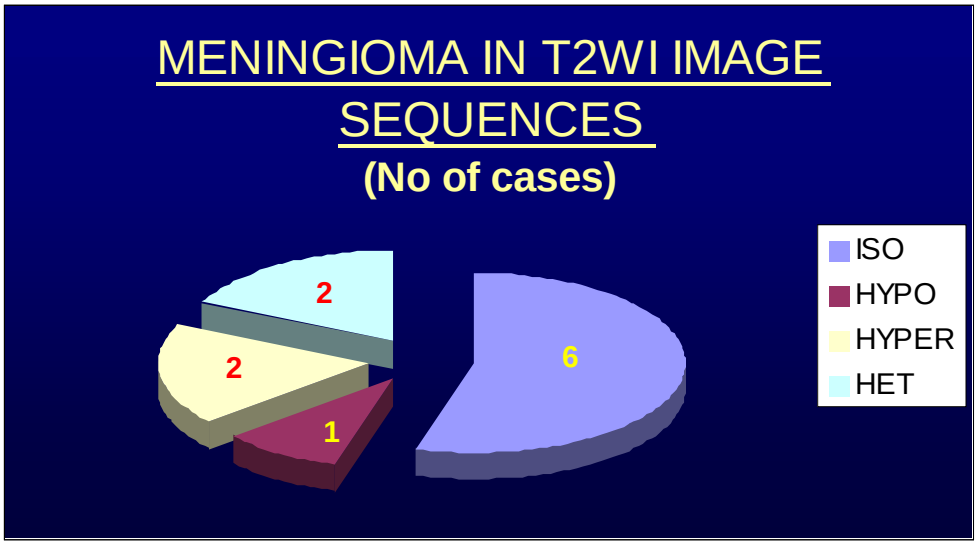

64% of meningiomas were iso to hypointense on T2WI.two cases were hyperintense on T2WI which were histologically turned out to be meningothelial type.

TABLE – 12
DIFFUSION RESTRICTION OF TUMOURS

TUMOURS	TOTAL NO OF CASES	NO RESTRICTION		RESTRICTION	
		CASES	%	CASES	%
GLIOMA	42	42	100%	-	-
MENINGIOMA	11	11	100%	-	-
SELLAR LESIONS	7	7	100%	-	-
MEDULLOBLATOMA	7	4	57%	3	43%
SCHWANNOMA	5	5	100%	-	-
ARACHNOID CYST	2	2	100%	-	-
EPIDERMOID CYST	2	0	-	2	100%
INTRAVENTRICULAR TUMOURS	4	4	100%	-	-

Diffusion restriction noted in epidermiod cysts 100% , medulloblatomas 42.8%.

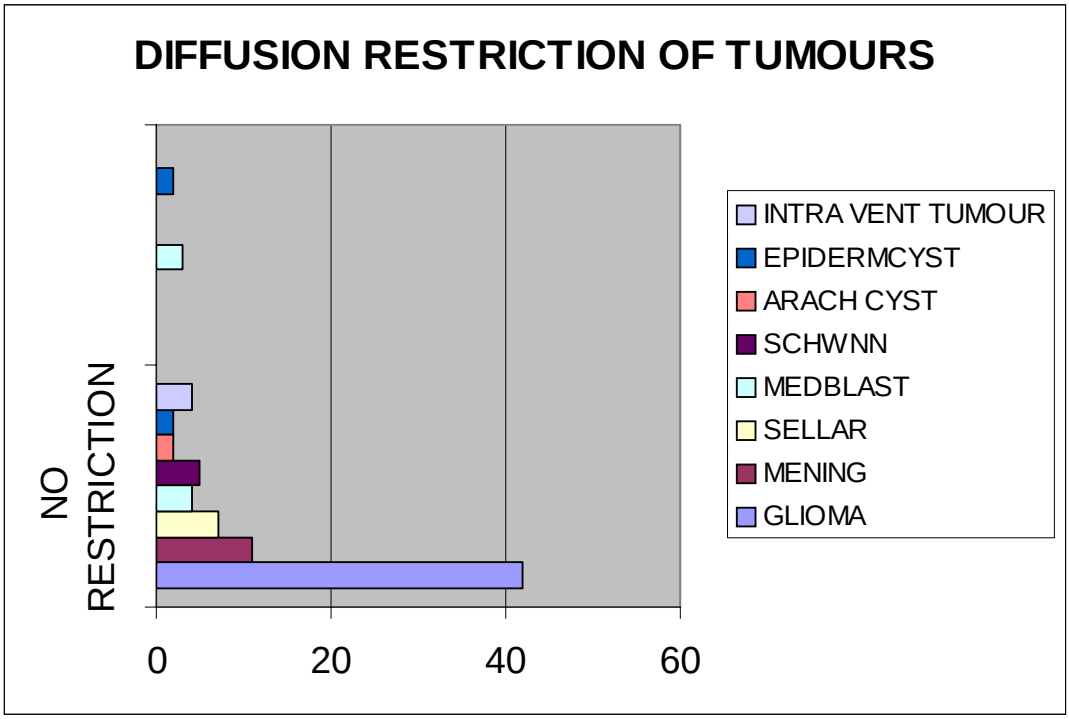

DISCUSSION

In our study of 80 patients, 52.5% were gliomas. Out of 42 cases of gliomas, 17 cases were glioblastoma multiforme ,11 anaplastic astrocytoma, 8 low grade astrocytoma, 4circumscribed astrocytoma, 2 were oligodendroglioma. The peak incidence of these tumours were 5^{th} and 6^{th} decade and male to female ratio is 1.47:1.

The incidence, peak age of presentation are comparable to De Jongh et al., 1978 and Silverman et al in 1981[18].

In our study of 17 cases of glioblastoma multiforme, all were heterointense on T1WI due to hemorrhage and necrosis. CT and MRI diagnosis was made in 15 cases of glioblastoma multiforme and other two appeared as anaplastic astrocytoma which were glioblastoma multiforme on HPE.

Of 11 cases of anaplastic astrocytoma, 1 case radiologically appeared as glioblastoma multiforme.

On contrast administration, no enhancement was noted in low grade astrocytomas. Enhancement was noted in 45.5% of anaplastic astrocytoma, 100% of glioblastoma multiforme. There is relationship of contrast enhancement and tumour grading noted in our study. All glioblastoma

multiforme cases showed intense enhancement of tumour margins (non necrotic areas).

This is comparable to the results of Earnest F IV, Scheithauer BW et al., in year 2000, in which the intensity of the enhancement is significant and correlates with the level of cellular anaplasia[19].

Hemorrhage was noted in 9 cases of 42 gliomas and all were glioblastoma multiforme.

So grading of malignancy using CT and MRI is 92%. Study of Dean B, Drayer B, Bird C et al in 1990 showed that the imaging features on CT & MRI, although generally correlating with tumour grade, are not entirely specific[20].

Calcification was noted in 14 cases out of 80 cases of primary brain tumours. In glioma of 42 cases only 5 (11.9%) showed calcification. In meningiomas of 11 cases, 3 (27.2%) showed calcification. All 3 cases of craniopharyngioma showed calcification.

Dense calcification noted in oligodendroglioma, mural nodule calcification was noted in pilocytic astrocytoma.

In three cases of craniopharyngioma all showed calcification in the solid component. One of two cases of central neurocytoma showed calcification.

LOW GRADE ASTROCYTOMA:

Incidence of low grade astrocytoma in our study was 10% of primary brain tumours.

Most cases displayed no mass effect, no calcification, no hemorrhage. No contrast enhancement noted.

Smirniotopoulus JG et al 1n 1999 showed that in low grade astrocytoma the contrast enhancement is usually absent reflecting a lack of tumour vascularity, blood brain barrier break down, or both. The above character is also noted in our study[21].

All lesions appeared hypointense on T1, most appeared hyperintense onT2 and showed no diffusion restriction. There was one false negative case in which radiologically appeared granulomatous lesion turned out to be low grade astrocytoma on HPE. Hence the sensitivity is 87.5% in diagnosing low grade astrocytoma by CT & MRI.

ANAPLASTIC ASTROCYTOMA:

Incidence of anaplastic astrocytoma in our study was 13.7% of primary brain tumours.

Peak age of incidence –4th and 5th decade.

Male: female ratio 1.2:1.

In our study anaplastic astrocytomas were ill defined, exhibited moderate mass effect.

Contrast enhancement noted in 5 cases. Calcification and hemorrhage were not seen. In MRI most lesion appear hetero intense on T2 WI. Out of 11 cases of anaplastic astrocytoma, 10 cases identified as anaplastic astrocytoma radiologically and one case reported as glioblastoma multiforme. Hence the sensitivity of CT & MRI in diagnosing AA is 90.9%.

GLIOBLASTOMA MULTIFORME:

Incidence of glioblastoma multiforme in our study was 21.2% of primary brain tumours.

Male: female ratio 1.4:1.

Peak age of incidence –5th and 6th decade

All the glioblastoma multiforme were ill defined in CT, exhibited more mass effect and heterogeneity and more vasogenic oedema. All showed areas of necrosis and hemorrhage which were clearly demonstrated on MRI. Calcification was noted in 1 case. Contrast enhancement was noted in all cases in non necrotic areas which was moderate to intense.

Butler AR, Horri SC et al., in their study showed that that contrast enhancement of viable tumour including the peripheral rim and the intratumoral solid portions is nearly universal in glioblastomas[22]. Our study also revealed the same feature.

Out of 17 cases of glioblastoma multiforme, 15 cases were diagnosed as glioblastoma multiforme and 2 cases were diagnosed as anaplastic astrocytoma. So, the sensitivity is 88.2% in diagnosing GBM.

OLIGODENDROGLIOMA:

Incidence of oligodendroglioma in our study is 2%.

Both the cases were hyperdense on plain CT with dense calcification and mild contrast enhancement and oedema. On MRI both the lesions were hetero intense on T1WI and T2 WI due to calcification. The diagnostic accuracy of oligodendroglioma in our study is 100%.

MENINGIOMAS:

They are the most common nonglial primary brain tumour. Most are homogeniusly hyperdense and densely enhances on contrast administration. According to Aronove et al ., in 1978 CT detects 85% and 95 % of cases in plain and contrast enhanced CT respectively.

Incidence of meningiomas in our study was 13.7% of primary brain tumours.

Male: female ratio 0.3 : 1 showing female predominance.

Peak age of incidence--5^{th} and 6^{th} decade.

Distribution of meningioma in our study :

Falx and convexity --7 cases (64%)

Supra sellar -- 2 cases

CP angle -- 2 cases

Naidich TP et al in 1990 in their study showed that the parasaggital region and the cerebral convexity are the common sites accounting for

nearly half of all meningiomas[23]. This same distribution pattern was seen in our study.

On plain CT 10 cases were homogenously hyperdense and one was isodense. Calcification noted in three cases 27.2 % and in CECT dense homogenous enhancement noted in all the cases. Dural tail was noted in 4 cases (36.3%).

Out of 11 cases of meniongima, correct diagnosis was made out in 10 cases, one was diagnosed radiologically as schwannoma which histologically turned out as meningioma. On MRI T2 WI most meningiomas appeared as iso to hypointense to the gray matter. Two cases appeared as hyperintense on T2WI which were meningothelial type of meningiomas on HPE. This is comparable with the study of Kaplan RD , Drayer BP et al., in year 1992 and Zee CS, Chin T et al in 1992 in which meningiomas with T_2 hyperintensity are of meningothelial type[24,25,26].

CIRCUMSCRIBED ASTROCYTOMA:

All the cases in our study were pilocytic astrocytomas, two were supratentorial and two were infratentorial in location. All showed large cystic component and a mural nodule. And two cases showed calcification of the mural nodule. All cases showed mural nodule enhancement as per the following study.

Luh GY, Bird CR *et* al in 1999 showed that typically after intravenous administration of contrast agent dense homogenous enhancement of tumour nodule but not of the other walls of the cyst[27].

MEDULLOBLASTOMA:

In our study there were 7 cases of medulloblastoma out of 80 cases of primary brain tumours. The incidence was 8.7%. Most appeared hyperdense on plain CT and showed moderate contrast enhancement. They appeared hypointense on T1WI and hyperintense on T2WI and FLAIR. Three cases out of 7 showed diffusion restriction.

This is comparable to the study of Rodallec M,Colombat M *et* al., in 2004 in which 2 cases showed diffusion restriction suggestive of small cell histology[28,29].

ACOUSTIC SCHWANNOMA:

In our study, 5 cases were acoustic schwannomas which showed acute angulation with the petrous ridge. and the incidence was 6%. Most of them isodense to the cortex on CT and all showed contrast enhancement. Most were hyopointense onT1WI and hyperintense on T2WI and FLAIR and showed no diffusion restriction.

TUMOURS OF SELLAR AND SUPRA SELLAR REGIONS:

Pituitary adenomas are the common lesions in the sella accounting for 10 % of all primary neoplasms as reported by Russel and Rubinstein *et* al., in 1989. In our study of 80 cases 4 cases were pituitary macro adenomas

and three were craniopharyngiomas. All the pituitary macraoadenomas enhanced well with contrast. And one showed carotid encasement. Most appeared hypointense on T1WI , slightly hyperintense on T2WI.

Incidence of craniopharyngioma in our study is 42% of sellar lesions. All occurred in children and all showed calcification. All showed heterointense signal in T1WI and T2WI due to cystic areas and calcification. All showed mild to moderate contrast enhancement (100%).

Johnsen DE Woodruff WW, Allen IS et al showed that of all the sellar region masses, craniopharyngiomas have the most heterogenous MR imaging spectrum[30,31].

ARACHNOID CYST:

Two cases were arachnoid cyst one in posterior fossa and the another was in right middle cranial fossa. Both of them followed CSF signal intensity in all pulse sequences and showed no diffusion restriction.

EPIDERMOID CYST:

There were two cases of epidermoid cysts in our study. One was located in the left cerebello pontine angle and another was in middle cranial fossa. Both the lesions appeared hypodense on CT. On MRI they appeared hypointense on T1WI and hyperintense on T2WI. Both the lesions were not suppressed on FLAIR and they showed diffusion restriction. There was no contrast enhancement in both the cases[32].

INTRAVENTRICULAR TUMOURS:

There were 4 cases of intraventricular tumours in our study. The incidence was 5%. Two cases located in the body of the lateral ventricle and both were central neurocytomas. Both the lesions appeared heterodense with lobulated 'bubbly' appearance. One showed calcification. There was mild contrast enhancement. On MRI they appeared heterointense and showed attachment to the septum pellucidum and mild contrast enhancement.

One case was choroid plexus papilloma situated in the atrium of the right lateral ventricle which was lobulated and isodense on CT. On MRI the lesion appeared isointense on T1WI & T2WI. On contrast there was intense contrast enhancement. There was communicating hydrocephalus clearly demonstrated by both CT & MRI.

Shoemaker EI, Gado M et al study showed that intense slightly heterogenous enhancement following contrast administration is seen in virtually in all choroid plexus papillomas[33].

Colloid cyst at the foramen of monro was well defined and hyperdense on plain CT. The lesion was hyperintense on T1WI and hypointense on T2WI. There was no contrast enhancement.

CONCLUSION

Computed tomography and magnetic resonance imaging are excellent modalities in diagnosis of primary brain tumours especially in tumour location and extent.

In majority of the cases, it is possible to arrive at a specific diagnosis based on CT & MRI characteristics.

With these modalities we can also guide the neurosurgeons to the ideal site of biopsy and to support in deciding the nature of therapy.

ANNEXURE

ABBREVIATION

AA	–	Anaplastic Astrocytoma
CT	–	Computed Tomography
CECT	–	Contrast Enhanced Computed Tomography
Ca^{++}	–	Calcification
Circ A	–	Circumscribed Astrocytoma
DWI	–	Diffusion Weighted Imaging
FLAIR	–	Fluid attenuation and Inversion Recovery Sequence
GBM	–	Glioblastoma multiforme
HPE	–	Histopathological examination
LA	–	Low Grade Astrocytoma
MRI	–	Magnetic Resonance Imaging
MRA	–	MR - Angiography
MRV	–	MR - Venography
MRS	–	Magnetic Resonance Spectroscopy
NECT	–	Nonenhanced Computed Tomography
ODG	–	Oligodendro Glioma
T_1WI	–	T_1 weighted imaging
T_2WI	–	T_2 weighted imaging
T_1C+	–	T_1 contrast

BIBLIOGRAPHY

1. Okazaki H : Neoplastic and Related conditions in Fundamentals of neuropathology, ed 2 , pp 203-274 , Tokyo 1989.

2. Stephen A. Kieffer Intracranial neoplasms in CT and MRI of whole body volume I, 4th edition , page 124.

3. Atlas SW, Lavi E, fisher PG: Intraaxial brain tumors, In atlas SW(ed): Magnetic resonance imaging of the brain and spine, 3rd Ed. Philadelphia, Lippincott Williams & Wilkins, 2002, pp 565-693.

4. Atlas SW, Lavi E, Goldberg HI: Extraaxial brain tumors. In Atlas SW (ed): Magnetic Resonance Imaging of the Brain and Spine, 3rd Ed. Philadelphia, Lippincott Williams & Wilkins, 2002, pp 695-772.

5. Baker HL Jr: The impact of computed tomography on neuroradiologic practice. Radiology 116: 637-740, 1975.

6. Baker HL JR, Campbell JK, Houser OW, et al: Computer assisted tomography of the Head: An early evaluation. Mayo Clin Proc 49: 17-27, 1974.

7. Wortzman G, Holgate Rc, Morgan PP: Cranial computed tomography: An evaluation of cost effectiveness. Radiology 117:75-77, 1975.

8. Brant – Zawadzki M et al. Primary intra cranial tumour imaging. A comparison of magnetic resonanace and CT. Radiology 150 : 435 – 440 , 1984.

9. Kwock L: Localized MR spectroscopy: Basic principles. Neuro imaging Clin North Am 8: 733-752, 1998.

10. Poptani H, Gupta RK et al: Characterization of intracranial mass lesions with in vivo proton MR splectroscopy. AJNR Am J Neuroradiology 16: 1593-1603, 1995.

11. Law M, Cha S, Knopp EA, et al: High grade gliomas and solitary metastases: Differentiation by using perfusion and proton spectroscopic MR Imaging: Radiology 222; 715-721, 2002.

12. Law M, Cha S, Knopp Ea, et al: High-grade gliomas and solitary metastases: Differentiation by using perfusion and proton spectroscopic MR imaging. Radiology 222: 715-721, 2002.

13. Di Chiro G, De La paz RL, Brooks RA, et al: Glucose utilization of cerebral gliomas measured by (18F) fluorodeoxyglucose and position emission tomography. Neurology 32: 1323-1329, 1982.

14. Stephen A. Kieffer Intracranial neoplasms in CT and MRI of whole body volume I, 4th edition , page 125.

15. Jelinek J, Smirniotopoulos JG, Parisi JE, Kanzer M: Lateral ventricular neoplasms of the brain: differential diagnosis based on clinical, CT, and MR findings, AJNR 11: 567-574, 1990.

16. Diagnostic Imaging brain - Anne G.Osborn M.D., F.A.C.R , Mosby year book 1st edition. Part I, section 6 pp 1-100.

17. Text Book of neurosurgery. B.Ramamurthi 2nd edition Churchill Livingstone 1996.

18. De Jongh, CT of supratentorial astrocytoma clinical neurology and neurosurgery: 1978, 60(3): 156- 68.

19. Earnest F IV, Kelly PJ, Scheithauer BW et al: Cerebral astrocytomas: Histopathological correlation of MR and CT contrast enhancement with sterotactic biopsy. Radiology 166: 823-827.

20. Dean B, Drayer B, Bird C et al in 1990 Gliomas : Classification with MR imagiong . Radiology 174: 411- 415.

21. Smirniotopoulos JG : The new WHO classification of brain tumours Neuro imaging Clin North AM , 9: 595 to 613 , 1999.

22. Butler Ar, Horii SC, Kricheff II, et al: computed tomography in astrocytomas: A statistical analysis of the parameters of malignancy and the positive contrast-enhanced Ct scan. Radiology 129: 433-439,1978.

23. Naidich TP: Imaging evaluation of meningiomas: categorical course on CNS neoplasms, American Society of Neuroradiology, 1990.

24. Kaplan RD, Coon S, Drayer BP et al: MR characteristics meningioma subtypes of 1.5 Tesla, J. Comp Asst. Temp 16: 366-371, 1992.

25. Zee CS, Chin T, Segall HD, Destian S, Ahmadi J. Magnetic resonance imaging of meningiomas.School of Medicine, University of Southern California, Los Angeles

26. Daemerel P, Wilms G, Lammeus M et al: Intracranial meningiomas: correlation between MR imaging and histology in fifty patients, J Comp Asst Tomogr 15:45-51, 1991.

27. Luh GY, Bird CR: Imaging of brain tumors in the pediatricpopulation. Neuroimaging Clin North Am 9: 691-716, 1999.

28. Kotsenas AL, Roth TC, Manness WK, Faerber EN. PUBMED
Abnormal diffusion-weighted MRI in medulloblastoma Pediatric Radiology. 1999 Jul; 29(7):524-6

29. Rodallec M, Colombat M, Krainik A, Kalamarides M, Redondo A, Feydy A Diffusion-weighted MR imaging and pathologic findings in adult cerebellar medulloblastoma. J Neuroradiol. 2004 Jun;31(3):234-7.

30. Johnsen DE, Woodruff WW, Allen IS et al: MR imaging of the sellar and juxtasellar regions, Radiographics 11: 727-758, 1991.

31. Schwartzberg DG: Imaging of pituitary tumors, Sem US, CT, MR 13: 207-223, 1992.

32. Diagnostic Imaging brain - Anne G.Osborn M.D., F.A.C.R , Mosby year book 1st edition. Part I, section 7 pp 16-20.

33. Shoemaker EI, Gad M choroid plexus papilloma , AJR 152: 1333-1338, year 1989.

34. Diagnostic radiology Grainger & Allison's – 4th edition Volume III

35. Diagnostic neuroradiology Anne G.Osborn M.D., F.A.C.R , Mosby year book 1st edition.

36. CT and MR imaging of the whole body John R. Haaga , M.D., F.A.C.R, Volume I, 4th edition.

PROFORMA

IMAGING OF PRIMARY BRAIN TUMORS

NAME:

AGE:

SEX:

WARD: UNIT: IP NO:

COMPLAINTS:

- Headache
- Projectile vomiting
- Neurological defecit
- Seizures

CLINICAL EXAMINATION:

- Motor system
- Sensory system
- Cerebellar system
- Fundus – papillodema

INVESTIGATIONS

CT

MRI

RADIOLOGICAL DIAGNOSIS

HPE DIAGNOSIS

MASTER CHART

S. No	Name	Age/Sex	Location	CT						MRI						Radiologic Diagnosis	HPE
				Margin	Density	Calcific	HE	Edema mass	Cont.	T_1	T_2	FLAIR	Diff	Edema Mass	Cont.		
1.	Ravi	35/M	Rt.Temporal	MD	Hypo	–	–	–	–	Hypo	Hyper	Het	–	–	–	LA	DA G II
2.	Srinivasalu	8/M	Pons	ID	Hypo	–	–	+	–	Hypo	Hyper	Het	–	+	–	LA	DA G II
3.	Govindasamy	48/M	Rt.Temporal	ID	Hypo	–	–	–	–	Hypo	Hyper	Hyper	–	–	–	LA	DA G II
4.	Gajendry	52/F	Lt. parietal	MD	Hypo	–	–	–	–	Hypo	Hyper	Hypo	–	–	–	LA	DA G II
5.	Saravanan	19/M	Rt. parietal	MD	Hypo	–	–	–	–	Hypo	Hyper	Hyper	–	–	–	LA	DA G II
6.	Ramalingam	24/M	Pons	MD	Hypo	–	–	+	–	Hypo	Hyper	Hyper	–	+	–	LA	DA G II
7.	Kannan	20/M	Lt. parietal	ID	Hypo	–	–	–	–	Hypo	Hyper	Hyper	–	+	–	Tuberculoma	DA G II
8.	Hemavathy	37/F	Rt. Frontal	ID	Hypo	–	–	–	–	Hypo	Hyper	Hyper	–	+	–	L.A	DA G II
9.	Kumar	32/M	Rt. TP	ID	Hypo	–	–	+	+	Hypo	Het	Het	–	+	+	AA	DA G III
10.	Thirunavokarasu	47/M	Lt. P	MD	Hypo	–	–	+	+	Hypo	Hyper	ISO	–	+	++	AA	DA G III
11.	Pandian	27/M	Rt. P	MD	Hypo	–	+	–	+	Het	Hyper	Het	–	+	++	AA	DA G III
12.	Kanniappan	65/M	Lt. Temporal	ID	Het	–	–	+	+	Hypo	Hyper	Hyper	–	+	+	AA	DA G III
13.	Subalakshmi	53/F	Rt.Frontal	ID	Hypo	–	–	+	+	Hypo	Het	Het	–	+	+	GBM	DA G III
14.	Sivaji	50/M	Lt. FP	ID	Hypo	–	–	+	–	Hypo	Hyper	Hyper	–	+	–	AA	DA G III
15.	Gopala Krishnan	45/M	Lt. PO	ID	Hypo	–	+	+	–	Hypo	Hyper	Hyper	–	+	–	AA	DA G III
16.	Sarasu	35/F	Rt. parietal	ID	Hypo	–	–	+	–	Hypo	Het	Het	–	+	–	AA	DA G III
17.	Uma	36/F	Lt. Parietal	ID	Hypo	–	–	+	–	Hypo	Het	Het	–	+	–	AA	DA G III

S. No	Name	Age/Sex	Location	CT						MRI						Radiologic Diagnosis	HPE
				Margin	Density	Calcific	HE	Edema mass	Cont.	T_1	T_2	FLAIR	Diff	Edema Mass	Cont.		
18.	Fahima	45/F	Rt.Temporal	ID	Hypo	–	–	+	–	Hypo	Het	Het	–	+	–	AA	DA G III
19.	Kanniammal	46/F	Lt.Temporal	ID	Hypo	–	–	+	–	Hypo	Het	Het	–	+	–	AA	DA G III
20.	Raja	25/M	Rt. Frontal	ID	Het	–	+	+	+	Hypo	Het	Het	–	+	++	GBM	DA G IV
21.	Sujatha	36/F	Bifrontal	ID	Het	–	+	+	++	Hypo	Het	Het	–	+	++	GBM	DA G IV
22.	Chandramouli	18/M	Bifrontal	ID	Hypo	–	+	+	++	Hypo	Hyper	Hyper	–	+	++	GBM	DA G IV
23.	Pandi	42/M	Lt. Frontal	ID	Hypo	+	–	+	+++	Het	Het	Het	–	+	+++	GBM	DA G IV
24.	Amudha	43/F	Bifrontal	ID	Hypo	–	–	+	++	Het	Het	Het	–	+	++	GBM	DA G IV
25.	Ramasamy	46/M	Lt. Parietal	ID	Hypo	–	+	+	+++	Het	Het	Het	–	+	+++	GBM	DA G IV
26.	Fathima	48/F	Rt. Parietal	ID	Hypo	–	–	+	++	Het	Het	Het	–	+	++	GBM	DA G IV
27.	Abdul	42/M	Lt. emporal	ID	Hypo	–	–	+	+++	Het	Het	Het	–	+	+++	GBM	DA G IV
28.	Victoria	43/F	Rt.Temporal	ID	Hypo	–	+	+	++	Het	Het	Het	–	+	++	GBM	DA G IV
29.	Christopher	51/M	Lt. Occipital	ID	Hypo	–	–	+	+++	Het	Het	Het	–	+	+++	GBM	DA G IV
30.	Malathy	52/F	Rt. Frontal	ID	Hypo	–	+	+	+	Het	Het	Het	–	+	+	AA	DA G IV
31.	John	53/M	Bifrontal	ID	Hypo	–	+	+	+++	Het	Het	Het	–	+	+++	GBM	DA G IV
32.	Chithirai	53/F	Bifrontal	ID	Hypo	–	–	+	++	Het	Het	Het	–	+	+++	GBM	DA G IV
33.	Malarkannan	55/M	Lt. Frontal	ID	Hypo	–	–	+	+++	Het	Het	Het	–	+	+++	GBM	DA G IV
34.	Ramalakshmi	56/F	Lt. Parietal	ID	Hypo	–	–	+	++	Het	Het	Het	–	+	+++	GBM	DA G IV
35.	Palani	62/M	Rt. Parietal	ID	Hypo	–	–	+	+++	Het	Het	Het	–	+	+++	GBM	DA G IV

S. No	Name	Age/Sex	Location	CT						MRI						Radiologic Diagnosis	HPE
				Margin	Density	Calcific	HE	Edema mass	Cont.	T_1	T_2	FLAIR	Diff	Edema Mass	Cont.		
36.	Arumugam	65/M	Rt. Temporal	ID	Hypo	–	–	+	+	Het	Het	Het	–	+	+	AA	DA G IV
37.	Sridhar	13/M	Lt. Parietal	MD	Hypo with Isodense nodule	–	–	+	+ mural	Hypo	Hyper	Hyper	–	+	+ Mural Nodule	PilocyticAstro	PilocyticAstro
38.	Prabhakaran	29/M	PF	MD	Hypo	–	–	+	+	Hypo	Hyper	–	–	+	++	Pilocytic Astro	PilocyticAstro
39.	Chitra	22/F	Rt. Parietal	MD	Hypo	+	–	+	+	Hypo	Hyper	Hypo	–	+	+	PilocyticAstro	PilocyticAstro
40.	Selvi	12/F	PF	MD	Hypo	+	–	+	+	Hypo	Hyper	Hypo	–	+	++	PilocyticAstro	PilocyticAstro
41.	Murugan	36/M	Rt. Frontal	MD	Hyper	++	–	+	+	Het	Het	Het	–	+	+	ODG	ODG
42.	Nallal	44/F	Lt. Frontal	MD	Hyper	++	–	+	+	Het	Het	Het	–	+	+	ODG	ODG
43.	Vasanthi	45/F	Lt. CP angle	MD	Hyper	+	–	–	++	Hypo	ISO	ISO	–	+	++	Meningioma	Meningioma
44.	Maheswari	26/F	Rt. Frontal convexity	MD	ISO	–	–	+	++	Hypo	ISO	ISO	–	+	++	Meningioma	Meningioma
45.	Muthusamy	52/M	High Parietal	WD	Hyper	–	–	+	++	Hypo	ISO	ISO	–	+	++	Meningioma	Meningioma
46.	Dhanavalli	37/F	Suprasellar	MD	Hyper	–	–	–	++	ISO	ISO	Hyper	–	–	++	Meningioma	Meningioma
47.	Vijaya	23/F	Convexity Lt. Parietal	MD	Hyper	++	–	+	+	Het	Het	Het	–	+	+	Calcified Meningioma	Meningioma
48.	Ramprasath	42/M	Rt. CP Angle	MD	Hyper	–	–	+	++	ISO	ISO	ISO	–	+	++	Schwannoma	Meningioma
49.	Alagu Selvam	52/M	Rt. Parietal Convexity	MD	Hyper	+	–	–	+++	Het	Het	Het	–	+	+++	Meningioma	Meningioma

S. No	Name	Age/Sex	Location	CT						MRI						Radiologic Diagnosis	HPE
				Margin	Density	Calcific	HE	Edema mass	Cont.	T_1	T_2	FLAIR	Diff	Edema Mass	Cont.		
50.	Banu	62/F	Falx	WD	Hyper	–	–	–	++	Hypo	Hypo	Hypo	–	+	+++	Meningioma	Meningioma
51.	Chitra	43/F	Falx	WD	Hyper	–	–	+	++	Hypo	ISO	ISO	–	+	+++	Menigioma	Menigioma
52.	Durga	48/F	Suprasellar	WD	Hyper	–	–	+	++	Hypo	Hyper	Hyper	–	+	++	Meningioma	Menigioma
53.	Ellammal	57/F	Falx	WD	Hyper	–	–	+	+++	Hypo	Hyper	Hyper	–	+	+++	Meningioma	Menigioma
54.	Tamilsevan	25/M	Sella	MD	Hypo	–	–	+	+++	ISO	ISO	ISO	–	+	+++	Pit. Macro adenoma	Pit. Macro adenoma
55.	Subashkumar	20/M	Sellar	WD	ISO	–	–	–	++	Hypo	Hyper	Hyper	–	–	++	Pit. Macro adenoma	Pit. Macro adenoma
56.	Lakshmi	30/F	Sella	MD	Hypo	–	–	–	+	Hypo	Hyper	Hyper	–	–	+	Pit. Macro adenoma	Pit. Macro adenoma
57.	Kavitha	28/F	Sella	MD	Hypo	–	–	–	+	Hypo	Hyper	Hyper	–	–	+	Pit. Macro adenoma	Pit. Macro adenoma
58.	Sugmaran	5/M	Suprasellar	MD	Het	++	–	+	+	Het	Het	Het	–	+	++	Cranio Pharyngioma	Cranio Pharyngioma
59.	Tamil Selvan	1/M	SupraSellar	WD	Hypo	+	–	–	++	Hypo	Het	Het	–	–	++	Cranio Pharyngioma	Cranio Pharyngioma
60.	Sangeetha	4/F	SupraSellar	MD	Het	+	–	+	+	Het	Het	Het	–	+	+	Cranio Pharyngioma	Cranio Pharyngioma
61.	Siva	11/M	PF	ID	Het	+	–	+	+	Het	Hyper	Hyper	+	+	++	Medullo Blastoma	Medullo Blastoma
62.	Purani	13/F	PF	MD	Hyper	–	–	+	++	Hypo	Het	Het	+	+	++	Medullo Blastoma	Medullo Blastoma
63.	Preethikumari	12/F	PF	MD	Hyper	–	–	+	++	Hypo	Hyper	Hyper	+	+	++	Medullo Blastoma	Medullo Blastoma

S. No	Name	Age/Sex	Location	CT						MRI						Radiologic Diagnosis	HPE
				Margin	Density	Calcific	HE	Edema mass	Cont.	T_1	T_2	FLAIR	Diff	Edema Mass	Cont.		
64.	Palpandian	17/M	Lt. cerebellar hemisph	MD	Het	–	–	+	+	Hypo	Hyper	Hyper	–	+	+	Medullo blastoma	Medullo Blastoma
65.	Rani	10/F	PF	ID	Hyper	+	–	+	++	Hypo	Hyper	Hyper	–	+	++	Medullo Blasma	Medullo Blastoma
66.	Sankaran	6/M	PF	MD	Hyper	–	–	+	++	Hypo	Hyper	Hyper	–	+	++	Medullo Blasma	Medullo Blastoma
67.	Balaji	8/M	PF	MD	Hyper	–	–	+	++	Hypo	Hyper	Hyper	–	+	++	Medullo Blastoma	Medullo Blastoma
68.	Amudha	40/F	Lt. CP angle	MD	ISO	–	–	+	++	Het	Hyper	Hyper	–	+	++	Acoustic Schvannoma	Acoustic Schvannoma
69.	Devaki	51/F	Lt. CP angle	ID	Hypo	–	–	+	+	Hypo	Het	Het	–	+	+	Acoustic schvannoma	Acoustic Schvannoma
70.	Rani	35/F	Rt. CP Angle	MD	ISO	–	–	+	++	Hypo	Hyper	Hyper	–	+	++	Acoustic Schwannoma with multiple meningioma	Acoustic Schwannoma
71.	Ramu	35/M	Rt. CP angle	MD	Het	–	–	+	+	Hypo	Hyper	Hyper	–	+	+	Acoustic Schwannoma	Acoustic Schwannoma
72.	Suresh	19/M	Lt. CP angle	MD	ISO	–	–	+	++	Hypo	Hyper	Hyper	–	+	++	Acoustic Schwannoma	Acoustic Schwannoma
73.	Reshma	9/F	Rt. Middle Cranial Fossa	WD	Hypo	–	–	–	–	Hypo	Hyper	Hypo	–	–	–	Arachnoid Cyst	Arachnoid Cyst
74.	Ramya	1/F	Post Fossa	WD	Hypo	–	–	–	–	Hypo	Hyper	Hypo	–	–	–	Arachnoid Cyst	Arachnoid Cyst

S. No	Name	Age/Sex	Location	CT						MRI						Radiologic Diagnosis	HPE
				Margin	Density	Calcific	HE	Edema mass	Cont.	T_1	T_2	FLAIR	Diff	Edema Mass	Cont.		
75.	Srivasan	55/M	Lt. CP angle	MD	Hypo	–	–	+	–	Hypo	Hyper	Hyper	+	+	–	Epidermoid cyst	Epidermoid cyst
76.	Muniyammal	40/F	Suprasellar	MD	Hypo	–	–	–	–	Hypo	Hyper	Hypo	+	–	–	Epidermoid cyst	Epidermoid cyst
77.	Suresh	23/M	Bodies lat ventricles	MD	Het	–	–	–	++	Het	Hyper	Het	–	–	++	Central Neurocytoma	Central Neurocytoma
78.	Sukumar	25/M	Bodies of Lat. vent	ID	Hetero	+	–	+	+	Hypo	Het	Het	–	+	+	Central Neurocytoma	Central Neurocytoma
79.	Sangeetha	5/F	Rt. Lat. Ventricle Atrium	Lobulated	ISO	–	–	Hydro cephalus	+++	ISO	ISO	ISO	–	Hydro Cephalus	+++	Chroid Plexus Papilloma	Chroid Plexus Papilloma
80.	Ramya	20/F	Foramen oif Monro	WD	Hyper	–	–	+	–	Hyper	Hypo	Hypo	–	+	–	Colloid Cyst	Colloid Cyst

KEY TO THE MASTER CHART

Location:

Rt- Right, Lt- left, CP- Cerebellopontine angle, TP- Temporo parietal region, PF- Posterior fossa,

Margins:

WD- well defined, MD- Moderately defined, ID- ill defined

Density:

Hypo – Hypodensity , Hyper – Hyperdensity, Het- heterodensity

ISO- Isodensity

Cont – Contrast

+ - Mild enhancement, ++ - Moderate enhancement,

+++ - Intense enhancement

T1,T2, FLAIR :

Hypo – Hypointensity, Hyper – Hyperintensity, Het- Heterointensity, Iso - isointensity.

Diff – Diffusion weighted imaging

Radiological diagnosis:

LA - Low grade astrocytoma

AA - Anaplastic astrocytoma

Astro - Astrocytoma

GBM - Glioblastoma Multiforme

Pit - Pituitary

ODG - Oligodendrglioma

DAG - Diffuse Astrocytoma Grade